

# On the nature of the radial orbit instability in spherically symmetric collisionless stellar systems

E. V. Polyachenko,<sup>1\*</sup> I. G. Shukhman<sup>2†</sup>

<sup>1</sup>*Institute of Astronomy, Russian Academy of Sciences, 48 Pyatnitskaya St., Moscow 119017, Russia*

<sup>2</sup>*Institute of Solar-Terrestrial Physics, Russian Academy of Sciences, Siberian Branch, P.O. Box 291, Irkutsk 664033, Russia*

Accepted Received

## ABSTRACT

We consider a two-parametric family of radially anisotropic models with non-singular density distribution in the centre. If highly eccentric orbits are locked near the centre, the characteristic growth rate of the instability is much less than the Jeans and dynamic frequencies of the stars (slow modes). The instability occurs only for even spherical harmonics and the perturbations are purely growing (aperiodic). On the contrary, if all orbits nearly reach the outer radius of the sphere, both even and odd harmonics are unstable. Unstable odd modes oscillate having characteristic frequencies of the order of the dynamical frequencies (fast modes). Unstable even harmonics contain a single aperiodic mode and several oscillatory modes, the aperiodic mode being the most unstable.

The question of the nature of the radial orbit instability (ROI) is revisited. Two main interpretations of ROI were suggested in the literature. The first one refers to the classical Jeans instability associated with the lack of velocity dispersion of stars in the transverse direction. The second one refers to Lynden-Bell’s orbital approach to bar formation in disc galaxies, which implies slowness and bi-symmetry of the perturbation. Oscillatory modes, odd spherical harmonics modes, and non-slow modes found in one of the models show that the orbital interpretation is not the only possible.

**Key words:** Galaxy: centre, galaxies: kinematics and dynamics.

## 1 INTRODUCTION

Spherical systems with predominance of eccentric orbits are subject to the so-called radial orbit instability (ROI) that leads to formation of non-spherical structures. These structures are naturally associated with the triaxial bulges and bars, observed in a variety of self-gravitating systems, where the eccentric orbits could occur as a result of the radial collapse in early stages of formation. Numerical simulations of collapsing systems have been carried out in Aguilar and Merritt (1990), Roy and Perez (2004), Trenti and Bertin (2006). In addition to these non-equilibrium systems, it is of interest to study the stability of *equilibrium* models that are used in modelling galaxies, globular and open clusters. The stability conditions may impose substantial restrictions on the allowed parameters of models.

By analogy with the well-known Ostriker–Peebles stability criterion for disk systems, Polyachenko and Shukhman (1981) proposed a global stability criterion for spherical sys-

tems,  $\zeta_{\text{crit}} = 2T_r/T_{\perp} > 1.7 \pm 0.25$ , where  $T_r$  and  $T_{\perp}$  are total kinetic energy of radial and transverse motion. Subsequently it was found that the specified range for  $\zeta_{\text{crit}}$  is not rigorously found. In particular, a critical value of  $\zeta$  for generalized polytropic models was found close to 1.4 (Fridman and Polyachenko, 1984, Barnes et al. 1986), or even 1 (Palmer and Papaloizou, 1987).<sup>1</sup> On the other hand, Osipkov–Merritt models give examples of systems that preserve initial spherical shape with  $\zeta_{\text{crit}}$  as much as 2.5 (Meza and Zamorano 1997). The most stable radially anisotropic configuration ( $\zeta_{\text{crit}} \approx 2.9$ ) were obtained by Trenti and Bertin (2006) in the numerical simulation of collisionless collapse. In the latest models, the stabilizing effect was due to the nearly isotropic core, while large anisotropy was achieved due to a strongly anisotropic shell.

Several mechanisms were proposed to explain ROI, among which we mention two. The first mechanism treats this instability as the Jeans instability of anisotropic

\* E-mail: epolyach@inasan.ru

† E-mail: shukhman@iszf.irk.ru

<sup>1</sup> Note that the result by Palmer and Papaloizou was questioned by Polyachenko et al. (2011).

medium, in which the velocity dispersion in the transverse direction cannot resist gravitational attraction (Polyachenko and Shukhman, 1972, 1981; Antonov, 1973, Barnes et al. 1986). The other mechanism supported by Merritt (1987, 1999), Saha (1991), Weinberg (1991), Palmer (1994), and others is claimed to be similar to bar formation in rotating discs described by Lynden-Bell (1979): this is a *tendency* of some orbits to line up in the direction of the bar that leads to increase of the density and potential perturbation.

A detailed exposition of the latter approach is given by Palmer (1994), who describes allowed mathematical simplifications of a general matrix equation for eigenoscillations to study instability under question. It was assumed that:

- The modes are even (even spherical harmonics  $l$ ), since the stellar orbits are symmetric with respect to the centre of the system.
- The modes are ‘slow’, i.e. the modes eigenfrequency  $\omega$  must be much smaller than the characteristic radial frequency of stars,  $|\omega| \ll \Omega_1$ . Under this condition, periods of stars will be much shorter than characteristic time of the instability, and the orbits can be regarded as separate objects.

These two features certainly narrow the range of possible unstable modes compared to the more general former approach, in which the frequencies  $\omega$  can be of the order of the radial frequency,  $|\omega| \sim \Omega_1$ . For convenience, we denote the two mechanisms as ‘Jeans’ and ‘Lynden-Bell’, but the primary difference is fastness and slowness of unstable modes. Besides the mentioned above restrictions, the ‘Lynden-Bell’ mechanism assumes that a radial part  $\chi(r)$  of the eigenfunction of the perturbed potential  $\delta\Phi(r, \theta, \varphi) = \chi(r) Y_l^m(\theta, \varphi)$  is nodeless.

In what follows we analyse the spectra of radially-anisotropic DFs of the form  $F(E, L)$  to answer the question whether only slow modes, or both types of modes are possible. We imply that all unstable non-radial modes are due to ROI, provided they are stabilized by decreasing the radial anisotropy. For the analysis we employ a two-parametric family of radially anisotropic models without central singularity (Polyachenko et al. 2013):

$$F(E, L) = \frac{N(q, L_T)}{4\pi^3 L_T^2} H(L_T - L) F_0(E),$$

$$F_0(E) = 2(1+q)(-2E)^q, \quad (1.1)$$

where  $H(x)$  is the Heaviside step function; parameters  $q \geq -1$ ,  $L_T \geq 0$ ;  $E$  is the energy and  $L$  is the absolute value of the angular momentum of individual stars,

$$E = \frac{1}{2}(v_r^2 + v_\perp^2) + \Phi_0(r), \quad L = rv_\perp.$$

In the distribution function (DF) (1.1), the gravitational potential  $\Phi_0(r)$  is set to zero on the sphere boundary; the boundary radius  $R$ , and the total mass  $M$  are unity;  $N(q, L_T)$  is the normalization constant.

In contrast to the well-known Osipkov–Merritt models (Osipkov, 1979; Merritt, 1985), and generalized polytropic models (Cumm, 1952)

$$F_{\text{GP}}(E, L) = C(s, q) L^{-s} (-2E)^q, \quad (1.2)$$

where  $-1 \leq q \leq 7/2$ ,  $-\infty < s < 2$ , our family of models (1.1) have two advantages needed for correct analysis of the

ROI: (i) the central density and the potential are finite, and (ii) for a wide range of parameter  $q$ , variation of parameter  $L_T$  transforms the system from isotropic to purely radial. A technical advantage is that the specific form of the  $L$ -dependence of the DF significantly simplifies a cumbersome numerical procedure of finding the eigenmodes.

Below we investigate the stability of two series of DF (1.1) with fixed values of the parameter  $q = 0$  and  $q = -1$ . A principal difference between the two is in the energy distribution of stars: the former one holds equipartition, while the latter is mono-energetic, since  $\lim_{q \rightarrow -1^+} F_0(E) = \delta(E)$  (see, e.g., Gelfand and Shilov, 1964). For highly radially anisotropic systems, models of  $q=0$  series have orbits with small apocentric distances (short needles) confined in the centre, where the characteristic orbital frequency  $\Omega_{\text{dyn}}$  is very large. In contrast, in mono-energetic models length of all highly eccentric orbits is nearly equal, and all stars can reach the outer radius of the system. We find that this feature results in a completely different character of the instability.

The plan of the paper is as follows. In Section 2 we provide a general matrix equation to determine the eigenfrequencies, and its special form for the series under consideration. In Section 3 we present results of calculations of eigenmodes. Finally, in section 4 we summarize the results and discuss the physical mechanisms of radial orbit instability.

## 2 MATRIX EQUATIONS

In this paper, we address the problem of stability by finding the eigenfunctions  $\chi(r)$  and the eigenfrequencies  $\omega$  of collisionless systems using matrix method. The method was first proposed by Kalnajs (1977) for disk systems. For spherical systems we are interested in a similar matrix equation, which was first obtained by Polyachenko and Shukhman (1981). Details of the derivation has been repeatedly given in the literature (see, e.g., Polyachenko and Shukhman, 1981; Weinberg, 1991; Bertin et al., 1994; Saha, 1991; Palmer, 1994), so here we only present the equation and explain the notations. The equation can be written as

$$\text{Det} \|\delta^{\alpha\beta} - \mathcal{M}^{\alpha\beta}(\omega)\| = 0, \quad \alpha, \beta = 1, 2, 3, \dots, \quad (2.1)$$

where matrix  $\mathcal{M}^{\alpha\beta}(\omega)$  is given by the following expression

$$\mathcal{M}^{\alpha\beta}(\omega) = -4\pi G (2\pi)^2 \sum_{l_1=-\infty}^{\infty} \sum_{l_2=-l_1}^l D_{l_1}^{l_2} \iint \frac{dE dL}{\Omega_1} \times$$

$$F(E, L) \left[ \Omega_{l_1 l_2} \frac{\partial}{\partial E} + l_2 \frac{\partial}{\partial L} \right] \left( \frac{L \psi_{l_1 l_2}^{\alpha\beta}}{\omega - \Omega_{l_1 l_2}} \right). \quad (2.2)$$

The integration in (2.2) is taken over the allowed domain  $\mathcal{D}$  of two-dimensional action sub-space  $(E, L)$ . This is the so-called ‘Lagrangian’ form of the matrix elements (see Appendix A). It is different from the more familiar ‘Euler’ form:

$$\mathcal{M}^{\alpha\beta}(\omega) = 4\pi G (2\pi)^2 \sum_{l_1=-\infty}^{\infty} \sum_{l_2=-l_1}^l D_{l_1}^{l_2} \iint \frac{dE dL}{\Omega_1(E, L)} \times$$

$$\psi_{l_1 l_2}^{\alpha\beta}(E, L) \frac{\Omega_{l_1 l_2}(E, L) \frac{\partial F}{\partial E} + l_2 \frac{\partial F}{\partial L}}{\omega - \Omega_{l_1 l_2}(E, L)}, \quad (2.3)$$

which can be formally obtained by integrating by parts and discarding the boundary terms. Note that ‘Euler’ form becomes incorrect for  $F(E, L)$  with an integrable singularity at the sub-space boundary. For our series of models, this occurs for  $q < 0$  at the boundary  $E = 0$ .

In equations (2.2) and (2.3) indices  $\alpha$  and  $\beta$  correspond to the expansion of the radial part of the potential  $\chi(r)$  and the radial part of the perturbed density  $\Pi(r)$  over the biorthogonal set:

$$\chi(r) = \sum_{\alpha} C^{\alpha} \chi^{\alpha}(r), \quad (2.4)$$

$$\Pi(r) = \frac{1}{4\pi G} \sum_{\beta} C^{\beta} \rho^{\beta}(r). \quad (2.5)$$

The perturbations are assumed to be independent of the azimuthal variable  $\varphi$ , since the eigenfrequencies of the perturbations  $\omega$  for spherically symmetric distributions  $F = F(E, L)$  are independent of the azimuthal number  $m$ . Therefore, instead of the angular dependence of the general form  $\delta\Phi = \chi(r) Y_l^m(\theta, \varphi) e^{-i\omega t}$ ,  $\delta\rho = \Pi(r) Y_l^m(\theta, \varphi) e^{-i\omega t}$ , one can consider simplified axisymmetric one  $\delta\Phi = \chi(r) P_l(\cos\theta) e^{-i\omega t}$ ,  $\delta\rho = \Pi(r) P_l(\cos\theta) e^{-i\omega t}$ . Here, functions  $\chi^{\alpha}(r)$  and  $\rho^{\alpha}(r)$  are related by the Poisson equation

$$\left[ \frac{d^2}{dr^2} + \frac{2}{r} \frac{d}{dr} - \frac{l(l+1)}{r^2} \right] \chi^{\alpha} = \rho^{\alpha}$$

and satisfy the so-called biorthonormal conditions,

$$\int_0^1 \chi^{\alpha}(r) \rho^{\beta}(r) r^2 dr = -\delta^{\alpha\beta}.$$

Note that  $\chi^{\alpha}$  and  $\rho^{\alpha}$  depend on the index  $l$ , but we omit it for brevity.

Subscripts  $l_1$  and  $l_2$  correspond to the decomposition

$$\delta\Phi(I_1, I_2, w_1, w_2) = \sum_{l_1 l_2} (\delta\Phi)_{l_1 l_2}(\mathbf{I}) \exp[i(l_1 w_1 + l_2 w_2)]$$

of the spatial dependence of the perturbed potential in harmonics of angular variables  $w_1$  and  $w_2$  conjugate to action variables  $I_1$  and  $I_2$ :

$$I_1 = \frac{1}{2\pi} \oint p_r dr = \frac{1}{\pi} \int_{r_{\min}}^{r_{\max}} \sqrt{2E - 2\Phi_0(r) - \frac{L^2}{r^2}} dr, \quad I_2 = L.$$

The radial angular variable  $w_1$  is related to the radius  $r$  as follows:

$$w_1 = \Omega_1 \int_{r_{\min}}^r \frac{dr'}{\sqrt{2E - 2\Phi_0(r') - L^2/r'^2}}.$$

An explicit expression for the angular variable  $w_2$  can be found in the mentioned above papers (e.g., Polyachenko & Shukhman, 1981). For the perturbations independent of the azimuthal variable  $\varphi$ ,  $\delta\Phi$  and  $\delta\rho$  do not depend on the angular variable  $w_3$ . Functions  $\Omega_{l_1 l_2}(E, L)$  denote linear combinations of orbital frequencies,  $\Omega_{l_1 l_2} \equiv l_1 \Omega_1 + l_2 \Omega_2$ , which are determined by:

$$\frac{1}{\Omega_1} \equiv \frac{1}{\pi} \int_{r_{\min}}^{r_{\max}} \frac{dr}{\sqrt{2E - 2\Phi_0(r) - L^2/r^2}},$$

and,

$$\frac{\Omega_2}{\Omega_1} = \frac{L}{\pi} \int_{r_{\min}}^{r_{\max}} \frac{dr}{r^2 \sqrt{2E - 2\Phi_0(r) - L^2/r^2}} \equiv \frac{\Delta\varphi}{\pi},$$

where  $\Delta\varphi(E, L)$  is the angular distance in the orbital plane between  $r_{\min}$  and  $r_{\max}$ . For highly eccentric orbits and non-singular unperturbed potentials – the cases in which we are interested in, this angle is close to  $\frac{1}{2}\pi$ , giving the frequency ratio  $\Omega_2/\Omega_1 \approx \frac{1}{2}$ . Such orbits, called 2:1-orbits, are slowly precessing ellipses symmetric relative to the centre.

The coefficients  $D_l^k$  are nonzero only for even  $|l - k|$  and equal

$$D_l^k = \frac{1}{2^{2l}} \frac{(l+k)!(l-k)!}{\left[ \left(\frac{1}{2}(l-k)\right)! \left(\frac{1}{2}(l+k)\right)! \right]^2}.$$

Finally,  $\psi_{l_1 l_2}^{\alpha\beta}(E, L) = \phi_{l_1 l_2}^{\alpha}(E, L) \phi_{l_1 l_2}^{\beta}(E, L)$ , where,

$$\phi_{l_1 l_2}^{\alpha}(E, L) = \frac{1}{\pi} \int_0^{\pi} \cos \Theta_{l_1 l_2}(E, L; w_1) \chi^{\alpha}[r(E, L, w_1)] dw_1,$$

and the angle  $\Theta_{l_1 l_2}(E, L, w_1)$  is defined by  $\Theta_{l_1 l_2}(E, L; w_1) = \Omega_{l_1 l_2} \frac{w_1}{\Omega_1} - l_2 \delta\varphi(E, L; w_1)$ , where

$$\delta\varphi(E, L, w_1) = L \int_{r_{\min}(E, L)}^{r(E, L, w_1)} \frac{dx}{x \sqrt{[2E + 2\Psi(x)] x^2 - L^2}}$$

is the angular distance between  $r_{\min}$  and the current radius  $r$ ; the relative potential  $\Psi(r) \equiv -\Phi_0(r) > 0$ .

### 3 RESULTS

Equilibrium models of  $q = 0$  and  $q = -1$  were analysed in detail in Polyachenko et al. (2013). In both cases, limiting models  $L_T = 0$  describe systems of purely radial orbits with global anisotropy  $\xi \equiv 1 - \zeta^{-1} = 1$ . Nearly radial models corresponding to small  $L_T$  have isotropic and almost homogeneous kernel with radius  $r_1 \sim L_T$ . Within this radius, the potential is almost constant:  $\Psi(r) = \Psi(0) + \mathcal{O}(r^2)$ ,  $\Psi(0) > 0$ . For  $r > r_1$ , the density and the potential vary as follows:

$$\rho \sim \frac{\Psi^{q+1/2}}{r^2}, \quad \Psi \sim \ln^n(1/r), \quad n = (1/2 - q)^{-1}.$$

#### 3.1 $q = 0$ series

The DFs  $F(E, L)$  in  $q = 0$  series are independent of the energy  $E$  and the angular momentum  $L$  within the allowed domain  $\mathcal{D}$ :

$$F(E, L) = \frac{N(0, L_T)}{2\pi^3} \frac{H(L_T - L)}{L_T^2} H(-2E). \quad (3.1)$$

For the chosen form of DF, the expression for matrix elements  $M^{\alpha\beta}(\omega)$  is particularly simple, since the two-dimensional integration over  $\mathcal{D}$  is reduced to one-dimensional integration along two boundary lines: the vertical  $0 < L < L_T$ ,  $E = 0$ , and the horizontal  $L = L_T$ ,  $E_c < E < 0$  (shown by thick lines in Fig. 1). The models become isotropic when the parameter  $L_T \geq 0.6682$  (Polyachenko et al., 2013).

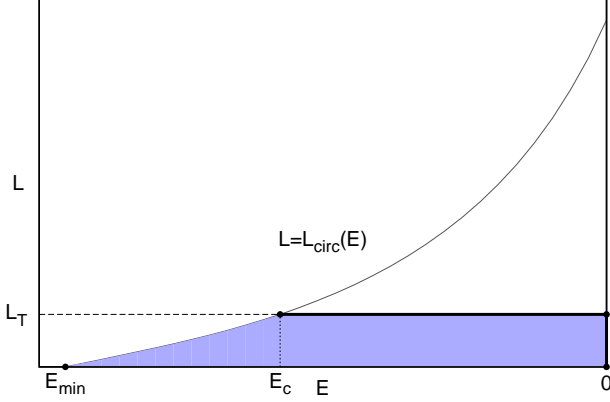


**Figure 1.**  $(E, L)$  sub-space and the allowed domain  $\mathcal{D}$  (filled area). The upper curve is the line of circular orbits.

A suitable expression for the matrix elements  $M^{\alpha\beta}(\omega)$  can be obtained from (2.3) and written in a form containing eigenfrequency squared and summation over non-negative  $l_1$  only:

$$M^{\alpha\beta}(\omega) = \frac{8N}{L_T^2} \int_0^{L_T} L dL S^{\alpha\beta}(0, L) - \frac{16N}{L_T} \sum_{l_1=0}^{\infty} S_{l_1} \sum_{l_2=-l_1}^l D_{l_2}^{l_1} \times \left\{ \frac{1}{L_T} \int_0^{L_T} L dL \frac{\omega^2 \psi_{l_1 l_2}^{\alpha\beta}(0, L)}{\Omega_{l_1}(0, L) [\omega^2 - \Omega_{l_1 l_2}^2(0, L)]} + \int_{E_c}^0 dE \frac{\Omega_{l_1 l_2}(E, L_T) \psi_{l_1 l_2}^{\alpha\beta}(E, L_T)}{\Omega_{l_1}(E, L_T) [\omega^2 - \Omega_{l_1 l_2}^2(E, L_T)]} \right\}. \quad (3.2)$$

Here, the coefficients  $S_{l_1} = 1/2$  for  $l_1 = 0$ , and  $S_{l_1} = 1$  otherwise. The first term on the r.h.s. of (3.2) results from a summation of terms independent of  $\omega^2$ :

$$S^{\alpha\beta}(E, L) = \frac{2}{\Omega_{l_1}(E, L)} \sum_{l_1=0}^{\infty} S_{l_1} \sum_{l_2=-l_1}^l D_{l_2}^{l_1} \psi_{l_1 l_2}^{\alpha\beta}(E, L),$$

which can be performed analytically (see, e.g., Saha 1991):

$$S^{\alpha\beta}(E, L) = \frac{1}{\pi} \int_{r_{\min}}^{r_{\max}} \frac{\chi^\alpha(r) \chi^\beta(r)}{[2E - 2\Phi_0(r) - L^2/r^2]^{1/2}} dr. \quad (3.3)$$

Using equations (2.1) with matrix elements (3.2), we investigate the stability of spherical harmonics  $l$  in the range  $1 \leq l \leq 20$  for  $L_T \geq 0.01$ . The model  $L_T = 0.01$  is highly radially anisotropic with ratio  $\zeta \equiv 2T_r/T_\perp = 42$ , and the global anisotropy  $\xi = 0.98$ .

Success of the matrix method depends largely on the appropriate choice of basis functions  $\{\chi^\alpha, \rho^\alpha\}$ . In Appendix B we describe a method for constructing a variety of basis sets in which  $\rho^\alpha = \lambda^\alpha g(r) \chi^\alpha$ , where function  $g(r)$  is arbitrary. The special case  $g(r) = -1$  corresponds to a well-known orthogonal system of spherical Bessel functions (Polyachenko and Shukhman, 1981).

A numerical code for mode's calculation was tested by finding lopsided  $l = 1$  shear modes, which is present in all models. They are called *zero modes*, since its eigenfrequency  $\omega = 0$ , and the eigenfunction  $\chi = \chi^1(r) = A\Psi'$ . Recall

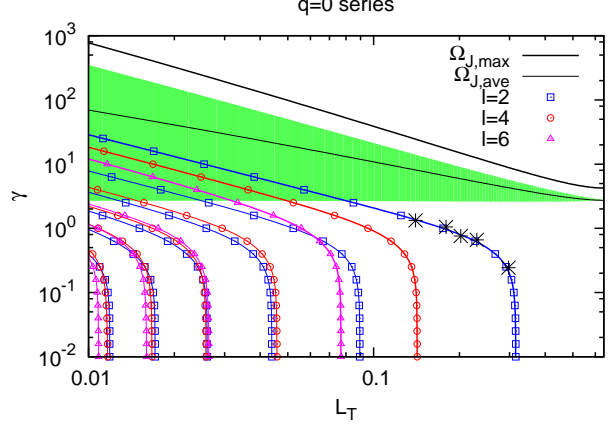


**Figure 2.** The dependence of the growth rate  $\gamma$  of aperiodic modes on the parameter  $L_T$  for  $l = 2, 4, 6$ . Stabilization of the most unstable mode  $l = 2$  occurs at  $L_{\text{crit}} = 0.316$ . Profiles of characteristic frequencies are given by (3.5). The shaded area shows the range of variation of the radial frequency  $\Omega_1$ ,  $(\Omega_J)_{\text{LOC}}$ , which almost coincides with the maximum radial frequency  $\Omega_1$  (not shown). Results of the growth rate  $N$ -body calculation for  $l = 2$  are given by asterisks.

that shift  $\delta z$  of the sphere as a whole along  $z$ -axis generates a perturbation of the potential  $\delta\Phi = \delta z \cdot \cos\theta \Phi'_0 \equiv \delta z \Phi'_0 P_1(\cos\theta)$ . For small  $\omega^2$ , the matrix elements can be represented as a series in  $\omega^2$ :

$$\mathcal{M}^{\alpha\beta}(\omega^2) = a^{\alpha\beta} + b^{\alpha\beta} \omega^2 + \mathcal{O}(\omega^4), \quad (3.4)$$

and hence  $\text{Det} \|\mathcal{M}^{\alpha\beta}(\omega^2) - \delta_{\alpha\beta}\| \approx A + B\omega^2$ . For the zero modes,  $A$  must vanish. In fact, it is not zero due to different approximations, such as, using a grid in  $(E, L)$  sub-space, substitution of the infinite matrix  $M^{\alpha\beta}$  by a matrix of finite size ( $N_\alpha \times N_\alpha$ ), and the replacement of an infinite series in  $l_1$  by finite series of length  $(l_1)_{\text{max}}$ . Assuming that an error is  $\delta\omega \equiv |A/B|^{1/2}$ , we can select the best basis by testing different functions  $g(r)$ . It turns out that for  $L_T = 0.1$  the appropriate choice is  $g(r) = -\rho(r)$ , with  $\delta\omega \approx 0.03$ . The zero mode test allowed us to verify the accuracy of the equations and obtain the accuracy estimate of eigenfrequency calculations. We also note that the accuracy drops sharply at  $L_T < 0.01$ .<sup>2</sup>

For  $g(r) = \rho'_0(r)/\Phi'_0(r)$ , the shear mode eigenfunction for the potential consists of only one element:  $\chi^\alpha(r) = A\Psi'(r)\delta^{1,\alpha}$ . So, all the elements in the first row and first column of matrix  $\mathcal{M}^{\alpha\beta}(0)$  must be close to zero, except that the first one is equal to unity.

The results of the stability study are the following.

1. There are no unstable solutions corresponding to odd spherical harmonics  $l$ .
2. For even values of  $l$  we found only *aperiodic* unstable solutions,  $\text{Re } \omega = 0$ ,  $\omega = i\gamma$ .
3. The unstable models are found within the range  $L_T < \dots$

<sup>2</sup> For very small  $L_T$ , we have developed recently a special approach which allows to investigate spectrum of eigenfrequencies even for almost pure radial models,  $L_T \rightarrow 0$ . This approach and its application will be presented in separate work.

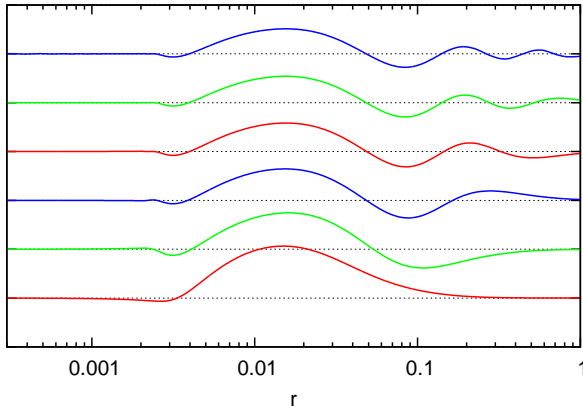


**Figure 3.** Radial profiles of the potential perturbation for the model  $L_T = 0.01$  corresponding to different modes of unstable spherical harmonic  $l = 2$ . To save room the profiles are shown in a single plot, but vertically separated from one another ( $\gamma_j$  decreases from bottom to top).

0.316, which corresponds to  $\zeta \equiv 2T_r/T_\perp > 2.2$ , or global anisotropy  $\xi > 0.55$ .

4. For a given spherical harmonic  $l$ , the number of unstable modes increases infinitely with decreasing  $L_T$ . These modes have different growth rates  $\gamma_j^{(l)}(L_T)$ ,  $j = 1, 2, \dots, j_{\max}^{(l)}(L_T)$  (see Fig. 2).

5. Eigenfunctions of the radial part of the potential perturbation, corresponding to different modes  $j$  differ in the number of nodes (see Fig. 3). Larger growth rates  $\gamma_j$  correspond to modes with fewer nodes.

6. With increasing  $L_T$ , the growth rates  $\gamma_j^{(l)}$  decrease, and modes with large number of nodes disappear.

Stabilization of all modes of  $l = 4$  harmonic occurs at  $L_T = 0.142$  ( $\zeta = 5.1$ ;  $\xi = 0.8$ ); all  $l = 6$  modes stabilize at  $L_T = 0.077$  ( $\zeta = 8.7$ ;  $\xi = 0.89$ ). The largest-scale nodeless mode ( $l = 2$ ) remains the most unstable for any value of parameter  $L_T < 0.316$ .

Fig. 2 compares the obtained growth rates of  $l = 2, 4, 6$  unstable modes, and some characteristic frequencies, such as radial frequency oscillations  $\Omega_1$ , and

$$\begin{aligned} (\Omega_J)_{\max} &= \sqrt{4\pi G\rho(0)}, \\ (\Omega_J)_{\text{ave}} &= \sqrt{4\pi G \int dr r^2 \rho^2(r)/M}, \\ (\Omega_J)_{\text{LOC}} &= \sqrt{4\pi G\rho(2r_1)}, \end{aligned} \quad (3.5)$$

where  $r_1$  is the isotropic radius of the nucleus.  $(\Omega_J)_{\text{ave}}$  is a weighted Jeans frequency;  $(\Omega_J)_{\text{LOC}}$  is a Jeans frequency on the radius of localization of the perturbation (i.e.,  $r_{\text{LOC}} \approx 2r_1$ ). It is seen that the growth rates are small compared with all characteristic frequencies (3.5): for instance,  $(\Omega_J)_{\text{LOC}}$  exceeds the growth rates for more than an order of magnitude.

The obtained slowness of the modes allows one to average over the motion of a particle along its orbit, and consider orbital slow dynamics rather than ordinary particle dynamics (see, e.g., Polyachenko, 2004, 2005). Then the matrix equation can be simplified, and instead of the full equation based on matrix (3.2), one may consider a ‘slow’ equation, which is obtained from (3.2) by omitting all terms except

those for which  $l_1 = -l_2/2$ . Similar simplification is used by Palmer (1994) for calculation and interpretation of the instability in the ‘Lynden-Bell’ approach. Recall that for highly eccentric orbits  $\Omega_2 \approx \Omega_1/2$ , which means

$$l_1\Omega_1 + l_2\Omega_2 = l_2(\Omega_2 - \frac{1}{2}\Omega_1) = l_2\Omega_{\text{pr}} \ll \Omega_{1,2}. \quad (3.6)$$

We checked the applicability of the ‘slow’ approach by direct recalculation of the spectra of modes for the lower spherical harmonics ( $l \leq 6$ ). The comparison demonstrates that difference in frequency values does not usually exceeds 1 per cent. Thus we conclude that for  $q = 0$  series ROI can be interpreted in terms of ‘Lynden-Bell’ mechanism.

This result seems suspicious in the absence of a dominant external potential, which provides a slow precession for all orbits and ensures the slow mode (Polyachenko et al., 2010). An order-of-magnitude estimate for eigenfrequencies gives the Jeans frequency, or the dynamical frequency,  $\omega \sim \Omega_J \sim \Omega_{\text{dyn}} \sim \sqrt{GM/R^3} = 1$ . However, this is a hasty conclusion: although the characteristic dynamical frequency is of the order unity, the maximum dynamical frequency of star oscillations ‘locked’ near the centre is very high. For  $q = 0$  series a large group of stars never leaves the centre, and despite the obtained growth rates are substantially greater than unity, they are still much smaller than the dynamical frequency of the locked stars. The slowness occurs here due to the small deviation of the potential from a harmonic form that exists in the central region. Note that these modes are turn out to be analogous to slow modes in near-Keplerian systems (Tremaine, 2001): in both cases orbital precession rates are low, and the modes are formed due to orbit-orbit alignment.

We performed an ‘experiment’ to determine which particles give the main contribution to the growth rates, retaining only contribution from  $E_c$  to some  $E = E_{\max} < 0$  in the integrals over the horizontal line  $L = L_T$ ,  $E_c < E < 0$ . Our calculations confirm that the main contribution to the matrix elements comes from particles with apocentric distances  $r_{\max}(E, L = L_T)$  much smaller than unity.

Jeans instability mechanism suggests a simple dependence of critical parameter  $(L_T)_{\text{crit}}$ , at which the system becomes stable, from the spherical harmonics  $l$ . For a system in equilibrium  $\sigma_r \sim R\sqrt{G\rho}$ , where  $\sigma_r$  is the radial dispersion. On the other hand, assuming marginal stability one can obtain for the Jeans characteristic scale in the transverse direction,  $\lambda_J$ , from the Jeans criterion  $\lambda_J \sim \sigma_\perp/\sqrt{G\rho}$ . Thus, using  $\lambda_J \sim R/l$ , we have

$$\frac{1}{l_{\text{crit}}} \sim \frac{\lambda_J}{R} \sim \frac{\sigma_\perp}{\sigma_r}, \quad (3.7)$$

which gives  $l_{\text{crit}} \sim (1 - \xi)^{-p}$  with the exponent  $p$  of order unity. Since for small  $L_T$ ,  $L_T \simeq (1 - \xi)(1/2 - q)$  (Polyachenko et al., 2013), it is natural to expect  $(L_T)_{\text{crit}}$  to be inversely proportional to some power of  $l$ :  $(L_T)_{\text{crit}} \propto l^{-1/p}$ .

Fig. 4 shows the stability boundaries  $(L_T)_{\text{crit}}$  for even harmonic numbers  $l$  in the range  $2 \leq l \leq 30$ . The filled circles show the results obtained using the full matrix equation (3.2). Starting from  $l = 10$ , the linear combination of orbital frequencies  $\Omega_{l_1 l_2} \equiv l_1\Omega_1 + l_2\Omega_2$  vanishes for some  $l_1, l_2$ . Due to these resonances, calculation of the stability boundaries becomes extremely time-consuming. Open circles show the results of calculations using the ‘slow’ equation, which are almost identical in the absence of resonances ( $l \leq 8$ ). How-

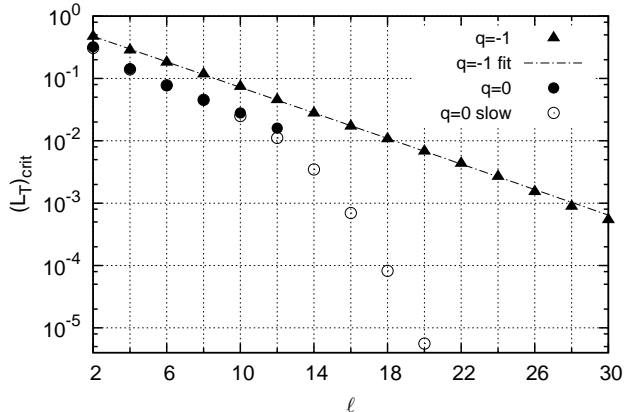


**Figure 4.** The dependence of the critical parameter  $(L_T)_{\text{crit}}$  on the harmonic number  $l$ :  $q = 0$  series (filled circles show the stability boundary inferred from the full integral equation (3.2), open circles from the ‘slow’ integral equation);  $q = -1$  series is shown by triangles (full equation). The dash-dotted line shows the least square linear fit to the  $q = -1$  boundaries.

ever, when resonances appear, the results begin to diverge. The full equation gives approximately exponential decay for  $(L_T)_{\text{crit}}(l)$ , while the ‘slow’ solution decreases significantly faster than exponent.

We conclude that the estimate for  $(L_T)_{\text{crit}}(l)$  based on usual Jeans relations for gravitating medium is incorrect to describe the bar-forming instability in highly heterogeneous systems. It enables only to predict the decrease with  $l$ . In addition, ‘slow’ solution is applicable only in the absence of resonances. Correct calculations of spherical harmonics  $l \geq 10$  are possible by using the full equation only.

Our matrix calculations was also supported by numerical  $N$ -body simulations using Superbox-10 code (Bien et al. 2013). This code is an example of a particle–mesh scheme, which solves the Poisson equation by fast Fourier transform. The number of grid points  $N_g$  for each coordinate is the same and is taken so that the number of grid cells be comparable with the number of particles. The number of particles in all calculations except one was  $10^6$ ; with  $N_g = 256$ . The model close to the stability limit ( $L_T = 0.2975$ ) was calculated with  $10^7$  particles and  $N_g = 512$ . The code uses three meshes. The biggest one allows us to simulate interaction between galaxies. Medium meshes are designed to simulate separate galaxies, and the smallest meshes are used to resolve fine structures in galactic centres. In all our calculations, the mesh sizes were taken to be 30, 5 and 1 (recall that the initial radius of the system  $R = 1$ ). The growth rates, evaluated from numerical experiments show good agreement with results of matrix calculations, especially for the models with moderate growth rates. On the other hand, in the models with  $L_T < 0.14$  it is difficult to distinguish the temporal interval of exponential growth of perturbations. This can be explained by interference of  $l = 2$  and  $l = 4$  modes. To investigate these models, initial states of high degree of symmetry as well as filtering of higher harmonics of force are needed.

### 3.2 $q = -1$ series

In contrast to  $q = 0$  series discussed above, models of  $q = -1$  series are monoenergetic, e.g. all stars have the same energy. In the limit of purely radial orbits all of them reach the outer radius; thus stars locked near the centre are absent. Accordingly, the dynamical frequencies of stars are almost identical and are of the order unity. Here we investigate how this affects the stability properties.

For the given  $q$ , the distribution function (1.1) reduces to:

$$F(E, L) = \frac{N(-1, L_T)}{4\pi^3} \frac{H(L_T - L)}{L_T^2} \delta(E), \quad (3.8)$$

where  $\delta(x)$  is the Dirac  $\delta$ -function. In the limiting case of purely radial orbits,  $L_T = 0$ , we obtain a model discussed by Agekyan (1962). On the other hand, systems become isotropic at  $L_T \geq 0.5613$ .

In the calculation of the matrix element,  $M^{\alpha\beta}(\omega)$ , two-dimensional integration is reduced to a one-dimensional integration over the vertical interval  $E = 0$ ,  $0 < L \leq L_T$ . However, the integrand includes a derivative with respect to energy, so some functions should be found in a small neighbourhood  $\Delta E < E < 0$ ,  $0 < L < L_{\text{circ}}(E)$ . The final expression of the matrix element obtained from (2.3) has a form:

$$M^{\alpha\beta}(\omega) = \frac{2N}{L_T^2} \frac{d}{dE} \left[ \int_0^{L_T} L dL \mathcal{S}^{\alpha\beta}(E, L) \right]_{E=0} - \frac{4N}{L_T} \sum_{l_1=0}^{\infty} S_{l_1} \times \sum_{l_2=-l}^l D_{l_1}^{l_2} \left\{ \left[ \frac{d}{dE} \int_0^{L_T} \frac{L dL}{L_T} \frac{\omega^2 \psi_{l_1 l_2}^{\alpha\beta}(E, L)}{\Omega_1(E, L) [\omega^2 - \Omega_{l_1 l_2}^2(E, L)]} \right]_{E=0} + \frac{\Omega_{l_1 l_2}(0, L_T) \psi_{l_1 l_2}^{\alpha\beta}(0, L_T)}{\Omega_1(0, L_T) [\omega^2 - \Omega_{l_1 l_2}^2(0, L_T)]} \right\}, \quad (3.9)$$

where  $\mathcal{S}^{\alpha\beta}(E, L)$  is defined by (3.3). The first term on the r.h.s. of (3.9) can be converted to

$$\frac{2N}{L_T^2} \frac{d}{dE} \left[ \int_0^{L_T} L dL \mathcal{S}^{\alpha\beta}(E, L) \right]_{E=0} = -\frac{2N}{\pi L_T^2} \times \left[ \int_{r_1}^{r_2} \frac{\chi^\alpha(r) \chi^\beta(r) r^2 dr}{\sqrt{2\Psi(r) - L_T^2/r^2}} - \int_0^1 \frac{\chi^\alpha(r) \chi^\beta(r) r^2 dr}{\sqrt{2\Psi(r)}} \right], \quad (3.10)$$

where in the first integral on the r.h.s. of (3.10)  $r_{1,2}$  are zeros of the radicand in the denominator.

Stability of individual harmonics is investigated by employing equation (2.1) with the matrix elements (3.9) for  $1 \leq l \leq 30$  and  $L_T \gtrsim 10^{-3}$ . Note that for the model with  $L_T = 0.01$ , parameter  $\zeta = 2T_r/T_\perp = 172$  and the global anisotropy  $\xi = 0.994$ .

The spectrum of unstable modes for models of this series differs significantly from the spectrum of  $q = 0$  series models. This applies to both even and odd spherical harmonics  $l$ .

1. For even  $l$ , there is only one aperiodic unstable mode,

$$\omega_0^{(l)}(L_T) = i\gamma_0^{(l)}(L_T)$$

and several oscillating unstable modes

$$\omega_j^{(l)}(L_T) = \bar{\omega}_j^{(l)}(L_T) + i\gamma_j^{(l)}(L_T), \quad j = 1, \dots, j_{\text{max}},$$

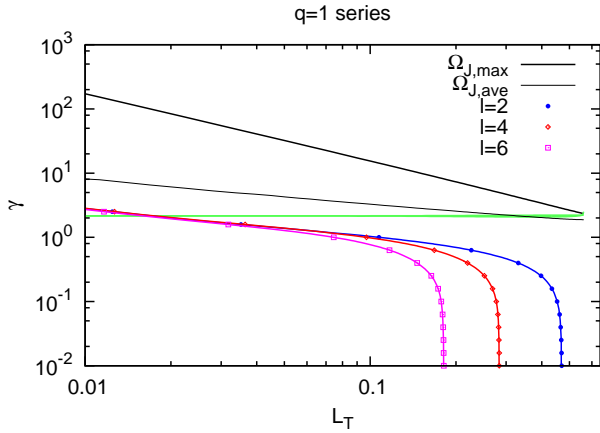


**Figure 5.** Same as in Fig. 2 for  $q = -1$  series. Stabilization of the most unstable mode  $l = 2$  occurs at  $L_{\text{crit}} \approx 0.47$ . The shaded area of  $\Omega_1$  variation is degenerated into a thin almost horizontal line.

in which the growth rates decrease with real part of the frequency increasing,

$$\bar{\omega}_{j-1}^{(l)}(L_T) < \bar{\omega}_j^{(l)}(L_T), \gamma_{j-1}^{(l)}(L_T) > \gamma_j^{(l)}(L_T),$$

and the number of unstable oscillatory modes  $j_{\text{max}}$  depends on  $L_T$ . The real parts of the frequencies are separated by  $\Omega_1$  (see Fig. 6 a):

$$\bar{\omega}_j^{(l)} - \bar{\omega}_{j-1}^{(l)} \approx \Omega_1(E = 0, L = L_T).$$

2. For odd modes starting with  $l = 1$ , there are only oscillating unstable modes, the real part of the frequencies are approximately equally spaced (see Fig. 6 b).

3. Growth rates of all modes decrease with increasing  $L_T$ . For a given even spherical harmonics  $l$ , less unstable oscillatory modes stabilize first, then more unstable aperiodic modes stabilize.

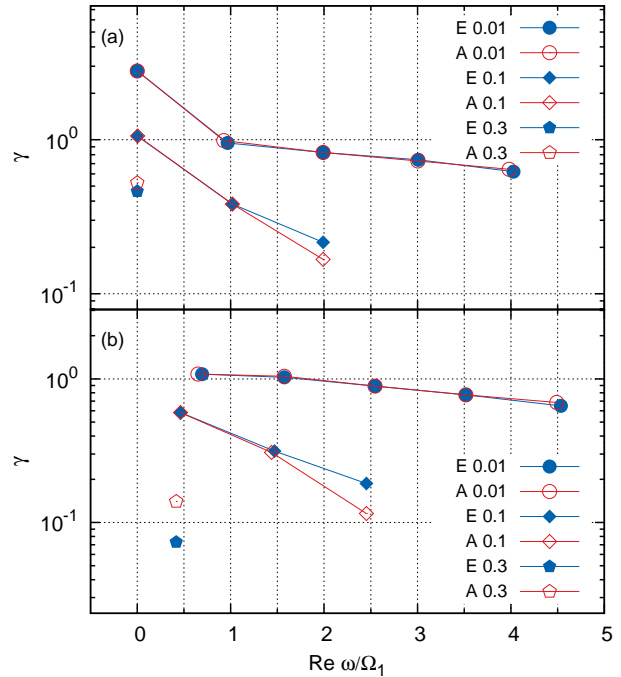
All non-spherical harmonics are fully stabilized when  $L_T > (L_T)_{\text{crit}} \approx 0.47$ , corresponding to  $\zeta < 1.5$  or  $\xi < 0.34$ . It coincides with the stabilization of aperiodic bar-mode instability,  $l = 2$  (see Fig. 5). Stabilization of  $l = 4$  harmonic occurs at  $L_T = 0.284$  ( $\zeta = 3.7$ ;  $\xi = 0.73$ ) and  $l = 6$  harmonic – at  $L_T = 0.182$  ( $\zeta = 6.9$ ;  $\xi = 0.85$ ).

Fig. 4 shows the stability boundary  $(L_T)_{\text{crit}}$  for even modes in the range  $2 \leq l \leq 30$ . The unstable modes (shown by triangles) are obtained using the full matrix equation (3.9). They fit well a simple relation:

$$\ln(L_T)_{\text{crit}} = -0.2359l - 0.2717.$$

Slight deviation from linearity at  $l \geq 26$  may be due to insufficient accuracy of the calculations.

Fig. 6 shows oscillatory and aperiodic modes of even harmonics for different values of  $L_T$ . Closed symbols show the solutions obtained using the full equation (3.9), whereas open symbols indicate eigenmodes found with a simplified equation derived from (3.9) by neglecting the terms associated with the energy derivative of the DF. The remaining last term in (3.9) mostly determines the eigenfrequencies, which also follows from the figure. For strongly radially anisotropic models, the growth rates of aperiodic modes are



**Figure 6.** The oscillating modes of  $q = -1$  series for three values of  $L_T$  ( $L_T = 0.01; 0.1; 0.3$ ): (a)  $l = 2$ , (b)  $l = 3$ . Solution (E) obtained by exact matrix equation (3.9); solution (A) by an approximate equation (see explanation in the text). All frequencies are given in units of the radial frequency for purely radial orbits  $\Omega_1 \approx 2.16$ .

much larger than unity. However, at  $L_T \gtrsim 0.1$  they become of the order unity and comparable with the growth rates of oscillatory modes. Note that the radial frequency  $\Omega_1(E, L)$  enters the equation at the boundary term  $E = 0$ ,  $L \leq L_T$  only, and for small  $L_T$  is close to a limit  $\Omega_1(0, 0) \approx 2.16$ . Thus, all the modes in this series can not be considered as slow ones.

Note that in contrast to  $q = 0$  models, in which some stars are locked in the centre, in  $q = -1$  models the orbits of stars have large radial excursions and are no longer in the regime of slow dynamics. This is a possible reason for the fastness of the  $q = -1$  modes.

## 4 CONCLUSION

This paper analyses two approaches presented in the literature to interpretation of the radial orbit instability (ROI). The first one explains ROI in terms of the classical Jeans instability. Indeed, it is natural to expect that radially anisotropic systems are ‘cold’ enough in the transverse direction for the instability to develop. Such an approach has been proposed in the first works devoted to ROI (Polyachenko and Shukhman 1972, 1981). The second approach appeals to a bar formation in disc galaxies proposed by Lynden-Bell (1979). His mechanism considers coalescence of the so-called ‘abnormal’ stellar orbits, for which the precession rates of stars,  $\Omega_{\text{pr}}$ , decreases with decrease of angular momentum  $L$  while the adiabatic invariant  $J_f = I_R + \frac{1}{2}L$  is conserved (here  $I_R$  is the radial action), i.e.  $(\partial\Omega_{\text{pr}}/\partial L)_{J_f} >$

0. Let a weak bar-like perturbation of the potential rotates at a slow rate  $\Omega_p$ . Orbits having a form of nearly symmetric ovals and the precession rates close to bar pattern speed effectively interact with the bar. The torque exerted by the bar on the abnormal orbit results in a change of the orbit precession rate, so that the orbit tends to line up with the bar, contributing to the potential well, thus enhancing the bar-like perturbations.

For spherical systems, highly eccentric orbits usually obey required inequality  $\partial\Omega_{pr}/\partial L > 0$ . Therefore, the idea of Lynden-Bell can allegedly be extended to spherical systems. However, the key assumption that makes this analogy legitimate is *slowness* of the perturbations, i.e. perturbation frequencies must be much smaller than the characteristic orbital frequencies. Otherwise, the concept of orbit as a separate united object (instead of a set of individual stars) interacting with potential perturbation is invalid. Moreover, the orbital approach can be used to describe symmetric relative to the center disturbances only. The easiest way to explain it is to consider perturbations on a disc, which have a form  $\delta\Phi \propto \cos(m\varphi)$ . Even  $m$  describe symmetric perturbations relative to the center, while for odd  $m$  signs of the potential are opposite at the opposite points:  $\Phi(r, \varphi + \pi) = -\Phi(r, \varphi)$ . In the latter case, the potential exerts differently on either side of the symmetric elliptic orbit. Note that for spherical models, the role of the azimuthal number  $m$  plays a spherical number  $l$ . If an unstable model violates any of these assumptions (the perturbation is not slow, or instability is possible for odd  $l$ ), then the validity of the ‘Lynden-Bell’ or, equivalently, ‘slow even- $l$ ’ or ‘orbital’) interpretation for this model can be put into question.

In this paper, we consider two series of DFs of the form  $F(E, L)$ . In the first one,  $q = 0$ , unstable perturbations are indeed slow, and are possible for even  $l$  only. In the second series,  $q = -1$ , the modes are fast, and instability is possible both for even and odd  $l$ . The reason for this difference is in the properties of energy dependence of their DFs. In the model with equipartition of the energy ( $q = 0$ ) many stars never leave the central region (their apocentric distances are much less than the radius of the system), where frequency of radial oscillations,  $\Omega_1$ , and Jeans frequency,  $\Omega_J$ , are much greater than frequencies of the perturbation. In this sense unstable modes are indeed slow, and thus the orbital approach to the instability is valid.

On the contrary, in the mono-energetic model ( $q = -1$ ) orbits of all stars nearly approach the outer radius, so our estimates that mode frequencies would be comparable to the characteristic dynamical frequency (almost the same for all stars) is proved true. Hence there is no way to use the orbital approach, and the odd modes obeying  $|\omega| \gtrsim \Omega_1$  can be excited.

We conclude that the spectra of radially-anisotropic DFs of the form  $F(E, L)$  are allowed to have both slow and fast modes. However, some DFs support essentially slow modes, while others allowing for both slow and fast modes.

## ACKNOWLEDGMENTS

The authors thank the referee for providing several valuable suggestions for presentation of the material, and Dr.

Jimmy Philip for editing the original version of the article that helped to improve its quality. This work was supported by Sonderforschungsbereich SFB 881 ‘The Milky Way System’ (subproject A6) of the German Research Foundation (DFG), RFBR grants No. 14-05-00080, 15-52-12387 and by Basic Research Program OFN-17 ‘The active processes in galactic and extragalactic objects’ of Department of Physical Sciences of RAS.

## REFERENCES

- Agekyan T. A., 1962, Vestnik Leningrad. Gos. Univ., Ser. math., mech., astr., No 1, 152 (in Russian)
- Aguilar L.A. and Merritt D. 1990, ApJ, 354, 33
- Antonov V. A., 1973, English translation in: de Zeeuw, T., ed. Proc. IAU Symp. 127, Structure and Dynamics of Elliptical Galaxies, Reidel, Dordrecht, p. 549
- Barnes J., Goodman J., Hut P., 1986, ApJ, 300, 112
- Bertin G., Pegoraro F., Rubini F., Vesperini E., 1994, ApJ, 434, 94
- Bien R., Brandt T., Just A., 2013, MNRAS, 428, 1631
- Cumm G.L., 1952, MNRAS, 112, 155
- Fridman A. M., Polyachenko V. L., 1984, Physics of Gravitating Systems. Springer, New York
- Gelfand I. M., Shilov G. E., 1964, Generalized functions. Academic Press, Inc.
- Kalnajs A.J., 1977, ApJ, 212, 637
- Lynden-Bell D., 1979, MNRAS, 187, 101
- Merritt D., 1985, AJ, 90, 1027
- Merritt D., 1987, IAUS, 127, 315
- Merritt D., 1999, PASP, 101, 129
- Osipkov L. P., 1979, Soviet Astron. Lett., 5, 42
- Palmer P. L., 1994, Stability of collisionless stellar systems: mechanisms for the dynamical structure of galaxies. Astrophysics and Space Science Library, Kluwer, Dordrecht, Boston
- Palmer P.L., Papaloizou J., 1987, MNRAS, 224, 1043
- Polyachenko E. V., 2004, MNRAS, 348, 345
- Polyachenko E. V., 2005, MNRAS, 357, 559
- Polyachenko E. V., Polyachenko V. L., Shukhman I. G., 2007, MNRAS, 379, 573
- Polyachenko V. L., Polyachenko E. V., Shukhman I. G., 2010, Astron. Lett., 36, 175
- Polyachenko E. V., Polyachenko V. L., Shukhman I. G., 2011, MNRAS, 416, 1836
- Polyachenko E. V., Polyachenko V. L., Shukhman I. G., 2013, MNRAS, 434, 3208
- Polyachenko V.L., Shukhman I.G., 1972, Preprint SibIZMIR 1-72
- Polyachenko V.L., Shukhman I.G., 1981, Sov. Astron. 25, 533
- Roy F., Perez J., 2004, MNRAS, 348, 62
- Saha P., 1991, MNRAS, 248, 494
- Tremaine S., 2001, AJ, 121, 1776
- Trenti M., Bertin G., 2006, ApJ, 637, 717
- Weinberg M.D., 1991, ApJ, 368, 66



## APPENDIX A: LAGRANGIAN FORM OF MATRIX EQUATION FOR SPHERICAL SYSTEMS

Matrix elements in equation (2.1) normally has the form

$$M^{\alpha\beta}(\omega) = 4\pi G (2\pi)^2 \sum_{l_1=-\infty}^{\infty} \sum_{l_2=-l_1}^l D_l^{l_2} \int \int \frac{dE L dL}{\Omega_1(E, L)} \psi_{l_1 l_2}^{\alpha\beta}(E, L) \frac{\Omega_{l_1 l_2}(E, L) \frac{\partial F}{\partial E} + l_2 \frac{\partial F}{\partial L}}{\omega - l_1 \Omega_{l_1 l_2}(E, L)}, \quad (\text{A1})$$

which is sometimes called ‘Euler’ form of the matrix elements. The matrix contains  $E$ - and  $L$ -derivatives of the DF  $F(E, L)$ . Our notations are explained in the main text.

Integration is taken over domain  $\mathcal{D}$  of the two-dimensional sub-space  $(E, L)$ , which depends on the DF. Boundaries of  $\mathcal{D}$  consist of line of circular orbits  $\ell_{\text{circ}}$ , line of radial orbits  $\ell_{\text{r.o.}}$ , and a line of escape  $\ell_{\text{singular}}$ , which is usually given by  $E = 0$ .

The Euler form of the matrix element has a significant drawback: if the DF  $F(E, L)$  is singular on any of the boundary lines (but the singularity is integrable), the Euler form contains divergent integrals. Note that two natural phase domain boundaries  $\ell_{\text{circ}}$  and  $\ell_{\text{r.o.}}$  are safe in this sense, because there is no flux through these lines (see below).

Our aim is to rewrite the Euler expression for the matrix element in the form that is free of  $E$ - and  $L$ -derivatives of the DF. For this we first write (A1) as follows

$$M^{\alpha\beta}(\omega) = 4\pi G (2\pi)^2 \sum_{l_1=-\infty}^{\infty} \sum_{l_2=-l_1}^l D_l^{l_2} \int \int \frac{dE L dL \psi_{l_1 l_2}^{\alpha\beta}(E, L)}{\omega - l_1 \Omega_1 - l_2 \Omega_2} \times \left\{ \frac{\partial}{\partial E} \left[ \left( l_1 + l_2 \frac{\Omega_2}{\Omega_1} \right) F \right] + \frac{\partial}{\partial L} \left( \frac{l_2}{\Omega_1} F \right) \right\}, \quad (\text{A2})$$

using the identity

$$\frac{\partial}{\partial E} \frac{\Omega_2}{\Omega_1} + \frac{\partial}{\partial L} \frac{1}{\Omega_1} = 0.$$

Now we introduce a ‘vector’  $\mathbf{A}_{l_1 l_2} = \left( (A_E)_{l_1 l_2}, (A_L)_{l_1 l_2} \right)$  with coordinates

$$(A_E)_{l_1 l_2} = \left( l_1 + l_2 \frac{\Omega_2}{\Omega_1} \right) F, \quad (A_L)_{l_1 l_2} = \frac{l_2}{\Omega_1} F,$$

and denote

$$B_{l_1 l_2}(E, L) = \frac{L \psi_{l_1 l_2}^{\alpha\beta}(E, L)}{\omega - l_1 \Omega_1 - l_2 \Omega_2}.$$

Then the integral

$$J_{l_1 l_2} \equiv \int \int \frac{dE L dL \psi_{l_1 l_2}^{\alpha\beta}(E, L)}{\omega - l_1 \Omega_1 - l_2 \Omega_2} \times \left\{ \frac{\partial}{\partial E} \left[ \left( l_1 + l_2 \frac{\Omega_2}{\Omega_1} \right) F \right] + \frac{\partial}{\partial L} \left( \frac{l_2}{\Omega_1} F \right) \right\} \quad (\text{A3})$$

can be written in the form:

$$J_{l_1 l_2} = \int \int dE dL B_{l_1 l_2} \operatorname{div} \mathbf{A}_{l_1 l_2} = \int \int dE dL \left[ \operatorname{div}(\mathbf{A}_{l_1 l_2} B_{l_1 l_2}) - (\mathbf{A}_{l_1 l_2} \nabla) B_{l_1 l_2} \right]. \quad (\text{A4})$$

According to the Gauss theorem

$$\int \int dE dL \operatorname{div}(\mathbf{A}_{l_1 l_2} B_{l_1 l_2}) = \int_{\ell} d\ell (\mathbf{A}_{l_1 l_2} B_{l_1 l_2}),$$

where  $\ell$  denotes the boundary of  $\mathcal{D}$ ,

$$\ell = \ell_{\text{circ}} + \ell_{\text{r.o.}} + \ell_{\text{singular}}.$$

The DF  $F(E, L)$  is allowed to be finite or to have integrable singularity on  $\ell_{\text{singular}}$ .

Vector  $\mathbf{A} \cdot \mathbf{B}$  vanishes on the boundary  $\ell_{\text{r.o.}}$ , as well as the vector flux across the boundary. This is due to the factor  $L$  in the expression for  $B_{l_1 l_2}$ . Furthermore, flux across the boundary  $\ell_{\text{circ}}$  vanishes due to the identity  $\phi_{l_1 l_2}^{\alpha}(E, L) \equiv \delta_{l_1 0} \chi^{\alpha}(R)$ , i.e. it vanishes on the circular orbits for all  $l_1$  and  $l_2$ , except  $l_1 = 0$ .

Yet, flux across  $\ell_{\text{singular}}$  is not zero, if DF takes finite values at this boundary. Moreover, the flux is infinite if the DF is singular on  $\ell_{\text{singular}}$ . To summarize,

$$\int_{\ell_{\text{circ}}} d\ell (\mathbf{A} \mathbf{B}) = 0, \quad \int_{\ell_{\text{r.o.}}} d\ell (\mathbf{A} \mathbf{B}) = 0, \quad \int_{\ell_{\text{singular}}} d\ell (\mathbf{A} \mathbf{B}) \neq 0.$$

Thus, the Euler form of the matrix element is invalid when the DF is singular but integrable on one of the boundary lines. Besides, non-integrable singularity is present in the integral (A1). We may conclude that standard linearization procedure is incorrect near the boundaries if one uses the Euler technique. It is therefore clear that the attempt to bring the Euler expression to valid (Lagrangian) form without derivatives of the DF by using the Gauss theorem (roughly, using integration by parts) was bound to fail.

The desired Lagrangian form could be obtained if the flux through  $\ell$  vanished. In this case, we have

$$J_{l_1 l_2} = - \int \int dE dL (\mathbf{A}_{l_1 l_2} \nabla) B_{l_1 l_2},$$

and for the matrix element:

$$M^{\alpha\beta}(\omega) = -4\pi G (2\pi)^2 \sum_{l_1=-\infty}^{\infty} \sum_{l_2=-l_1}^l D_l^{l_2} \int \int \frac{dE dL}{\Omega_1} F(E, L) \times \left[ \Omega_{l_1 l_2} \frac{\partial}{\partial E} + l_2 \frac{\partial}{\partial L} \right] \left( \frac{L \psi_{l_1 l_2}^{\alpha\beta}}{\omega - \Omega_{l_1 l_2}} \right). \quad (\text{A5})$$

However, to obtain this (correct) form, one needs to use the Lagrangian technique from the very beginning. It was first presented in the works by Kalnajs (see, e.g. Kalnajs, 1977). Rewriting a matrix element for disks (equation (16) of his paper) to the spherical geometry (in which we are interested in) one can have for the perturbations which are independent on the azimuthal angle  $\varphi$ :

$$M^{\alpha\beta}(\omega) = -4\pi G \frac{2l+1}{2} \sum_{l_1} \sum_{l_2} \int \int \int dI_1 dI_2 dI_3 F(E, L) \times \left( l_1 \frac{\partial}{\partial I_1} + l_2 \frac{\partial}{\partial I_2} \right) \left[ \frac{\Psi_{l_1 l_2}^{\alpha\beta}(I_1, I_2, I_3)}{\omega - \Omega_{l_1 l_2}(I_1, I_2)} \right]. \quad (\text{A6})$$

Here  $I_1$  is the radial action,  $I_2 = L$ ,  $I_3 = L_z$ ,  $\Omega_{1,2} = \partial E(I_1, I_2) / \partial I_{1,2}$ ,  $\Omega_3 = 0$ . Expression  $\Psi_{l_1 l_2}^{\alpha}(I_1, I_2, I_3)$  denotes

$$\Psi_{l_1 l_2}^{\alpha\beta}(I_1, I_2, I_3) = \Phi_{l_1 l_2}^{\alpha}(I_1, I_2, I_3) [\Phi_{l_1 l_2}^{\beta}(I_1, I_2, I_3)]^*, \quad (\text{A7})$$

where  $\Phi_{l_1 l_2}^\alpha(I_1, I_2, I_3)$  can be written in the form (see also Appendices in Polyachenko et al., 2007, Polyachenko and Shukhman, 1981)

$$\Phi_{l_1 l_2}^\alpha(E, L, \theta_0) = 2\pi P_l^{l_2}(0) P_l^{-l_2}(\sin \theta_0) e^{il_2\pi} \phi_{l_1 l_2}^\alpha(E, L), \quad (\text{A8})$$

where  $\sin \theta_0 = L_z/L$ ,  $-\frac{1}{2}\pi < \theta_0 < \frac{1}{2}\pi$ . From (A7) and (A8) one finds

$$\Psi_{l_1 l_2}^{\alpha\beta}(I_1, I_2, I_3) = (2\pi)^2 P_l^{l_2}(0) P_l^{-l_2}(\sin \theta_0) e^{il_2\pi} \phi_{l_1 l_2}^\alpha(E, L) \times P_l^{-l_2}(0) P_l^{l_2}(\sin \theta_0) e^{-il_2\pi} \phi_{-l_1, -l_2}^\beta(E, L). \quad (\text{A9})$$

or

$$\Psi_{l_1 l_2}^{\alpha\beta}(I_1, I_2, I_3) = (2\pi)^2 P_l^{l_2}(0) P_l^{-l_2}(\sin \theta_0) \times P_l^{-l_2}(0) P_l^{l_2}(\sin \theta_0) \psi_{l_1 l_2}^{\alpha\beta}(E, L). \quad (\text{A10})$$

Then one needs to change the differentiation with respect to actions  $I_1$  and  $I_2$  to differentiation with respect to  $E, L, \theta_0$  in (A6):

$$l_1 \frac{\partial}{\partial I_1} + l_2 \frac{\partial}{\partial I_2} = \Omega_{l_1 l_2} \frac{\partial}{\partial E} + l_2 \left[ \frac{\partial}{\partial L} - \frac{\sin \theta_0}{L} \frac{\partial}{\partial(\sin \theta_0)} \right],$$

transform the volume element  $dI_1 dI_2 dI_3 = dE L dL d(\sin \theta_0)/\Omega_1$ , and integrate over  $z \equiv \sin \theta_0$ . Since  $P_l^{l_2}(\pm 1) = 0$  provided  $l_2 \neq 0$ , and

$$\int_{-1}^1 dz z d[P_l^{l_2}(z) P_l^{-l_2}(z)] dz = - \int_0^1 dz P_l^{l_2}(z) P_l^{-l_2}(z),$$

then

$$\int_{-1}^1 dz \left( \frac{\partial}{\partial L} - \frac{z}{L} \frac{\partial}{\partial z} \right) \Psi_{l_1 l_2}^{\alpha\beta}(E, L, z) = \left( \frac{\partial}{\partial L} + \frac{1}{L} \right) \int_{-1}^1 dz \Psi_{l_1 l_2}^{\alpha\beta}(E, L, z). \quad (\text{A11})$$

Given that the integral over  $z$  is

$$\int_{-1}^1 dz P_l^{l_2}(0) P_l^{-l_2}(z) P_l^{-l_2}(0) P_l^{l_2}(z) = [2/(2l+1)] D_l^{l_2},$$

one finds

$$\int_{-1}^1 \Psi_{l_1 l_2}^{\alpha\beta}(E, L, z) dz = (2\pi)^2 \frac{2}{2l+1} D_l^{l_2} \psi_{l_1 l_2}^{\alpha\beta}(E, L). \quad (\text{A12})$$

Substituting (A12) into the r.h.s. of (A11), and then substituting the resulting expression in (A6), we obtain

$$M^{\alpha\beta}(\omega) = -4\pi G \frac{2l+1}{2} \sum_{l_1} \sum_{l_2} \int \int \frac{dE L dL}{\Omega_1} F(E, L) \times \left[ \Omega_{l_1 l_2} \frac{\partial}{\partial E} + l_2 \left( \frac{\partial}{\partial L} + \frac{1}{L} \right) \right] \frac{\int_{-1}^1 dz \Psi_{l_1 l_2}^{\alpha\beta}(E, L, z)}{\omega - \Omega_{l_1 l_2}}. \quad (\text{A13})$$

Finally, we have the desired expression of the matrix element in the Lagrangian form:

$$M^{\alpha\beta}(\omega) = -4\pi G (2\pi)^2 \sum_{l_1=-\infty}^{\infty} \sum_{l_2=-l}^l D_l^{l_2} \int \int \frac{dE dL}{\Omega_1} F(E, L) \times \left( \Omega_{l_1 l_2} \frac{\partial}{\partial E} + l_2 \frac{\partial}{\partial L} \right) \left( \frac{L \psi_{l_1 l_2}^{\alpha\beta}}{\omega - \Omega_{l_1 l_2}} \right). \quad (\text{A14})$$

## APPENDIX B: CONSTRUCTION OF THE BIORTONORMAL BASIS SETS

The effectiveness of the matrix method (2.1) depends on the proper choice of a basis function set  $\{\chi^\alpha(r), \rho^\alpha(r)\}$ ,  $\alpha = 1, 2, \dots$  satisfying the requirement of orthogonality:

$$\langle \chi^\alpha \rho^\beta \rangle \equiv \int_0^1 \chi^\alpha(r) \rho^\beta(r) r^2 dr = -\delta^{\alpha\beta} \quad (\text{B1})$$

and the Poisson equation:

$$\left[ \frac{d^2}{dr^2} + \frac{2}{r} \frac{d}{dr} - \frac{l(l+1)}{r^2} \right] \chi^\alpha(r) = \rho^\alpha(r). \quad (\text{B2})$$

This basis is used in expansion of the perturbation potential and density (2.5).

Instead of (B2), let us consider the following eigenvalue problem, assuming  $l \geq 1$ :

$$\left[ \frac{d^2}{dr^2} + \frac{2}{r} \frac{d}{dr} - \frac{l(l+1)}{r^2} \right] \chi(r) = \lambda g(r) \chi(r), \quad (\text{B3})$$

with boundary conditions

$$\chi(0) = 0, \quad \chi'(1) + (l+1)\chi(1) = 0. \quad (\text{B4})$$

The solution is a discrete set of positive eigenvalues,  $\lambda^\alpha$ , and eigenfunctions,  $\chi^\alpha(r)$ , orthogonal with weight  $r^2 g(r)$ :

$$\int_0^1 dr r^2 g(r) \chi^\alpha(r) \chi^\beta(r) \propto \delta^{\alpha\beta}. \quad (\text{B5})$$

Then the biortonormal set consists of functions  $\chi^\alpha(r)$  for the potential and functions  $\rho^\alpha = \lambda^\alpha g(r) \chi^\alpha(r)$  for the density. According to (B5), the biortonormal condition (B1) will be satisfied if the normalization of the functions  $\chi^\alpha(r)$  obeys

$$\lambda^\alpha \int_0^1 dr r^2 g(r) [\chi^\alpha(r)]^2 = -1. \quad (\text{B6})$$

In particular, for  $g(r) = -1$  we obtain the well-known biorthogonal basis:

$$\chi_l^\alpha(r) = \frac{\sqrt{2}}{\varkappa_\alpha} \frac{1}{|J_{l+1/2}(\varkappa_\alpha)|} \frac{J_{l+1/2}(\varkappa_\alpha r)}{\sqrt{r}}, \quad (\text{B7})$$

$$\rho_l^\alpha(r) = -\frac{\sqrt{2} \varkappa_\alpha}{|J_{l+1/2}(\varkappa_\alpha)|} \frac{J_{l+1/2}(\varkappa_\alpha r)}{\sqrt{r}}, \quad (\text{B8})$$

where  $\varkappa_\alpha$  are the positive roots of  $J_{l-1/2}(\varkappa_\alpha) = 0$ ,  $\alpha = 1, 2, \dots$  (Polyachenko, Shukhman 1981).

Choice of  $g(r) = \rho'_0(r)/\Phi'_0(r)$  is interesting for calculating the shear zero mode  $l = 1$ , with the perturbed potential and density, respectively,  $\chi(r) = \Phi'_0(r)$ , and  $\Pi(r) = \rho'_0(r)$ . The expansion for (2.5) contains only one term corresponding to the minimum eigenvalue  $\lambda = \lambda^{\alpha=1} = 4\pi$  (i.e.,  $C^1 = 1$ ;  $C^k = 0$  for  $k > 1$ ) and the basis function  $\chi^1(r) = \Phi'_0(r)$ .

Note that Bertin et al. (1994) discuss a similar technique for infinite systems. However, there is no attempt to build a system so that the expansion of the potential for shear mode contains a single function (which is useful for tests).

The eigenvalue problem (B3) in the form of a differential equation can be reduced to a more convenient eigenvalue problem in the form of an integral equation. In doing so, we write the equation (B3) in the equivalent form:

$$\chi(r) = -\frac{\lambda}{2l+1} \int_0^1 dr' r'^2 g(r') \chi(r') \mathcal{F}_l(r, r'), \quad (\text{B9})$$

where  $\mathcal{F}(r, r') = r_{<}^l / r_{>}^{l+1}$ ;  $r_{<} = \min(r, r')$ ,  $r_{>} = \max(r, r')$ . In this form, the boundary conditions are satisfied *automatically*.

Note that construction of a basis set for radial perturbations ( $l = 0$ ) is not covered by above analysis, and should be discussed separately.